

# Fluorescence correlation spectroscopy of gold nanoparticles, and its application to an aptamer-based homogeneous thrombin assay

Zhancheng Xu · Xiangyi Huang · Chaoqing Dong · Jicun Ren

Received: 30 July 2013 / Accepted: 15 November 2013 / Published online: 28 November 2013  
© Springer-Verlag Wien 2013

**Abstract** We have studied the fluorescence properties and diffusion behaviors of gold nanoparticles (GNPs) in solution by using fluorescence correlation spectroscopy (FCS) at single molecule level. The GNPs display a high photo-saturation feature. Under illumination with strong laser light, they display higher brightness per particle (BPP) despite their low quantum yields. Based on the unique fluorescence properties and diffusion behaviors of GNPs, we have developed a sensitive and homogenous thrombin assay. It is based on a sandwich strategy and is making use of GNPs to which two different aptamers are conjugated. When the differently aptamer-labeled GNPs are mixed with solutions containing thrombin, the affinity reaction causes the GNPs to form dimers or oligomers. This leads to an increase in the diffusion time of the GNPs in the detection volume that is seen in FCS. The FCS method enables sensitive detection of the change in the characteristic diffusion time of the GNPs before and after the affinity reaction. Quantitative analysis of thrombin is based on the measurement of the change in the diffusion time. Under optimal conditions, the calibration plot is linear in the 0.5 nM to 110 nM thrombin concentration range, and the detection limit is 0.5 nM. The method was successfully applied to the direct determination of thrombin in human plasma.

**Keywords** Gold nanoparticles · Fluorescent correlation spectroscopy · Brightness per particle · Thrombin · Aptamers

**Electronic supplementary material** The online version of this article (doi:10.1007/s00604-013-1132-2) contains supplementary material, which is available to authorized users.

Z. Xu · X. Huang · C. Dong · J. Ren (✉)  
College of Chemistry & Chemical Engineering, State Key  
Laboratory of Metal Matrix Composites, Shanghai Jiaotong  
University, 800 Dongchuan Road, Shanghai 200240, People's  
Republic of China  
e-mail: jicunren@sjtu.edu.cn

## Introduction

Fluorescent analysis is one of very important analytical methods, and is widely used in chemical, biological and biomedical fields due to its ultra-high sensitivity and good selectivity [1]. However, the sensitivity of fluorescent methods is dramatically dependent on the chemical and physical properties of labeling probes. Currently, the most commonly used optical labels are organic fluorescent dyes. Fluorescent dye probes possess small molecular weight and mature labeling technique, but their drawback is limited observation time owing to rapid photobleaching, which restricts their applications in some fields [2]. Recently, some nanoparticles are used as labeling probes in optical analysis and bioimaging, which mainly include quantum dots (QDs) [3], metal clusters, gold nanoparticles (GNPs) [4] and so on. Although QDs have high brightness per particle (BPP) and photostability over organic dyes [5], they are still unsuitable for some *in vivo* applications due to their certain degree of photodecomposition, certain biological toxicity and difficulty in functionalizing in a controlled way [6]. Generally, metal (gold or silver) clusters are composed of several to tens of metal atoms, and possess higher fluorescence efficiency (up to 10 %), but their chemical and fluorescence instability limits their application to cell or tissue imaging [7].

When compared to other fluorescent materials, GNPs (several tens nm) show certain advantages such as ease of synthesis, nonblinking, nonphotobleaching, simplicity of conjugation chemistry and excellent biocompatibility. More important, GNPs possess very strong light scattering and absorption properties [8]. Due to their excellent features, GNPs as probes have been used in chemical analysis, bioassays, single particle tracking, and bioimaging [9, 10]. So far, colorimetric and scattering detections are mostly used in GNPs-based heterogeneous immunoassays and DNA hybridization [11]. Among these applications, optical signal is mostly based on the fact

that GNPs resonantly scatter light upon excitation of the surface plasmon, and the scattering signal must be discriminated from the strong background, especially in cells or scattering tissue [12]. Generally, the selectivity of colorimetric and scattering detection methods is not as good as fluorescent method.

In fact, GNPs also possess fluorescence property, however, mainly because of their low quantum yields (QYs), these fluorescent GNPs do not attract great attention, and to date there were a few reports on the fluorescent features of GNPs [13–21]. Recently, we studied the fluorescent properties of colloidal GNPs with sizes between 20 and 80 nm by fluorescent imaging technique, and observed that these GNPs showed excellent behaviors of anti-photobleaching, and higher BPP under stronger light illumination. So far, we did not fully understand the fluorescent property of GNPs in solution, especially fluorescent feature of GNPs at the single particle level. In addition, there were few reports on the applications of fluorescent GNPs as fluorescent probes.

We investigated the fluorescent property of GNPs in solution by using single molecule spectroscopy-fluorescence correlation spectroscopy (FCS). We found that GNPs showed a high photo-saturation feature, and under illumination of stronger light, GNPs possessed a stronger BPP and non photobleaching. Furthermore, we investigated the diffusion behaviors of GNPs with different diameters in solution, and observed that the characteristic diffusion time was proportional to the diameters of GNPs. Based on the fluorescent properties and diffusion behaviors of GNPs, we developed a new homogenous method for determination of thrombin in human plasma by using FCS technique. Although certain methods have been developed for assay of thrombin, which include fluorescence [22], surface enhanced Raman scattering (SERS) [23], and electrochemistry [24], sensitive, simple and rapid assay of thrombin is still needed in clinical diagnosis. In the procedure for assay of thrombin, GNPs modified with aptamer were used as fluorescent probes, and sandwich strategy was used. This new method was successfully applied for determination of thrombin level in human plasma.

## Experimental

### Chemicals and reagents

Aptamer-1 (5'-HS-(CH<sub>2</sub>)<sub>6</sub>-TTTTTTTTTGGTTGGTGTGGTTGG-3') and aptamer-2 (5'-HS-(CH<sub>2</sub>)<sub>6</sub>-TTTTTAGTCGTGGTAGGGCAGGTTGGGGTGGACT-3') were provided by Sangon Biotech Co., Ltd. (Shanghai, China, <http://www.sangon.com>). A series of GNPs (20 nm, 40 nm, 60 nm and 80 nm) were purchased from Ted Pella, Inc., (USA, <http://www.tedpella.com>). Thrombin and bovine serum albumin

(BSA) were purchased from Sigma-Aldrich Chemical Co. (Milwaukee, USA, <http://www.sigmaaldrich.com>). Sodium citrate, disodium hydrogen phosphate, sodium dihydrogen phosphate and hydrogen tetrachloroaurate (III) hydrate (HAuCl<sub>4</sub>) were products from Sinopharm Chemical Reagent Co., Ltd. (Shanghai, China, <http://www.sinoreagent.com.cn>). All aqueous solutions were prepared with ultra-pure water (18.2 MΩ) which was obtained from the Millipore Simplicity System (Millipore Inc., Bedford, MA, USA, <http://www.millipore.com>).

Four human plasma samples from healthy subjects were provided by Hospital of Shanghai Jiaotong University, and were stored at -20 °C for further use. All experiments were performed in compliance with the relevant laws and institutional guidelines.

### Apparatus

Laser-induced fluorescence spectra of GNPs were recorded on a LabRAM spectrometer (HR 800, Jobin Yvon, France) with an Ar<sup>+</sup> laser (514.5 nm) as the excitation source. A temperature-controlled high-speed centrifuge was purchased from Beckman Coulter (USA, <http://www.beckmancoulter.com>). SPH-103B small capacity constant temperature shaker was obtained from Shanghai Shi Ping Experiment Equipment Co., Ltd. (Shanghai, China, <http://shipping.bioon.com.cn>). Transmission electron micrograph (TEM) images were taken with a JEM-2100 transmission electron microscope (Jeol-Ltd., Tokyo, Japan, <http://www.jeol.co.jp/en>).

FCS measurements were performed on a home-built FCS system [25] which is based on an inverted microscope (IX 71, Olympus, Japan <http://www.olympus-global.com/en>) and a 532 nm laser (SDL-532-LN-030T, Shanghai Dream Lasers Technology Co., Ltd., Shanghai, China, <http://www.dreamlasers.com>). The setup of FCS is shown in Fig. 1S. The 532 nm laser beam was reflected by a dichroic mirror (570DRLP, Omega Optical, Inc., USA, <http://www.omegafilters.com>), then focused into the sample solution by a water immersion objective (UplanApo, 60 × NA1.2, Olympus, Japan, <http://www.olympus-global.com/en>). The excited fluorescence signal which was collected by the objective passed through the dichroic mirror and two band-pass filters (605DF50 and BA590, Omega Optical, Inc., USA, <http://www.omegafilters.com>). As a difference from other FCS system, two band-pass filters were used here to block scattering laser light from the strong scattering signal of GNPs. Finally, the fluorescence signal was collected after passing a 35 μm pinhole by an avalanche photodiode (SPCM-AQR14, Perkin-Elmer EG&G, Canada, <http://www.perkinelmer.com>). The yielded signals were tracked and correlated by a real time correlator (Flex02-12D/C, USA, [correlator.com](http://www.correlator.com)). The measuring time per sample was 120 s.

FCS data analysis

All obtained FCS data were analyzed with the standard equation for particles diffusing in a three-dimensional Gaussian volume element and nonlinearly fitted with the Origin 6.1 software package based on the Levenberg-Marquardt algorithm [26]. This fit is based on the following model:

$$G(\tau) = \frac{1}{N} \cdot \frac{1}{\left(1 + \frac{\tau}{\tau_D}\right)} \cdot \frac{1}{\sqrt{1 + \left(\frac{\omega_{xy}}{\omega_z}\right)^2 \cdot \frac{\tau}{\tau_D}}} \quad (1)$$

Where  $N$  is average number of particles in the confocal detection volume,  $\tau_D$  is the characteristic diffusion time, and  $D$  is diffusion coefficient of particles. Here  $\omega_{xy}$  and  $\omega_z$  are radii of the laser focus in the XY-direction and Z-direction, respectively, at the  $e^{-2}$  point of the Gaussian laser beam intensity. The hydrodynamic radius  $R$  of GNPs can be calculated by Stokes-Einstein Eq. (3).

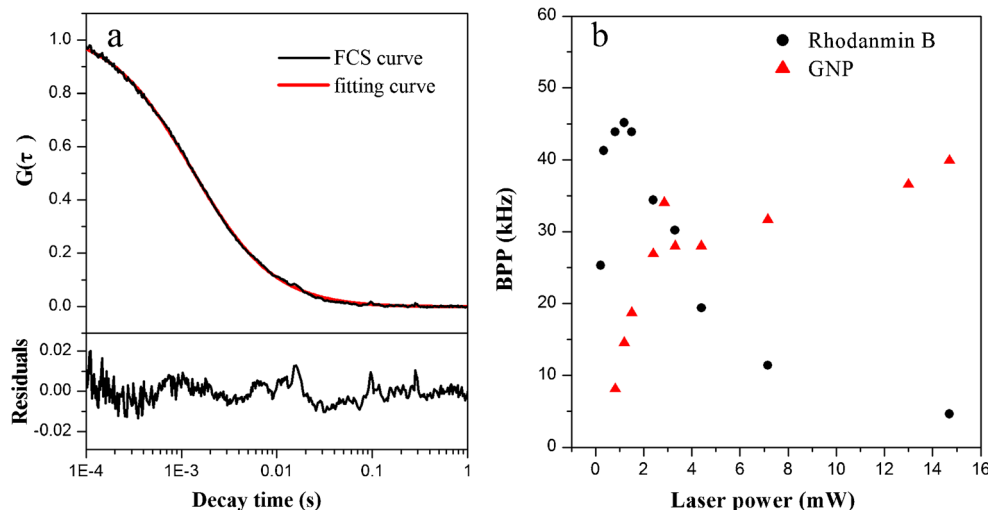
$$\tau_D = \frac{\omega_{xy}^2}{4D} \quad (2)$$

$$D = \frac{k_B T}{6\pi\eta R} \quad (3)$$

$$\tau_D = \frac{3\pi\eta\omega_{xy}^2 R}{2k_B T} \quad (4)$$

Where  $k_B$  is Boltzmann constant,  $T$  expresses solution temperature, and  $\eta$  is the viscosity of the solution. Under the given conditions,  $T$ ,  $\eta$  and  $\omega_{xy}$  are constants, and the characteristic diffusion time  $\tau_D$  should be proportional to hydrodynamic radius  $R$ .

**Fig. 1** Normalized autocorrelation curve of 30 nm GNPs and effects of illumination light intensity. **a** Normalized FCS curve, fitting curve and fitting residual curve of 30 nm GNPs (340 pM). Laser power was 3 mW (930 kW cm<sup>-2</sup>), and the measurement time was 120 s. **b** The effects of illumination light intensity on the fluorescent emission of GNPs and fluorescent dye (Rhodamine B). Two nM of Rhodamine B and 340 pM of 30 nm GNPs were used in this study



Synthesis and characterization of GNPs

GNPs (30 nm) were synthesized by reduction of the HAuCl<sub>4</sub> solution with sodium citrate and the synthesis method was described in the reference with a minor modification [27]. Briefly, 100 mL of 0.01 % (w/v) of the HAuCl<sub>4</sub> solution was heated to boiling for 15 min, and then 1 % (w/v) sodium citrate solution was added. Heating continued for 15 min after the solution color remained unchanged. After cooling down to room temperature, the prepared GNPs stock solution was stored at 4 °C for further use. The concentration of GNPs was 340 pM, which was calculated according to the method described in the reference [28].

Preparation of GNP-aptamer probes

Four hundred μL of 30 nm GNPs (340 pM) were added into a polypropylene tube, then pH of the GNPs solution was adjusted to 8.0 with 100 mM NaOH solution. Then 20 μL of aptamer-1 (10 μM) was added into the tube. The mixture was cultured at 25 °C for 24 h in a thermostatic shaker. After the reaction, 20 μL of NaCl solution (1 M NaCl, 0.1 M PBS buffer, pH=7.4) was added into the tube, then the mixture was kept at 4 °C for 8 h salinization. After salinization, 4 μL of 1 % (w/v) BSA solution was added into the tube, then the solution was slowly shaken at 25 °C for 1 h. The GNP-aptamer-1 probes were purified from excess aptamers by centrifugation at 5,000 rpm for 8 min, and then were washed once. The GNP-aptamer-1 probes were finally diluted to 50 μL and stored at 4 °C for immediate use. The GNP-aptamer-2 probes were prepared as the same procedure of GNP-aptamer-1 probes.

Procedure for assay of thrombin

Ten μL standard sample of thrombin solution (different concentrations), 5 μL GNP-aptamer-1 probes, 5 μL GNP-

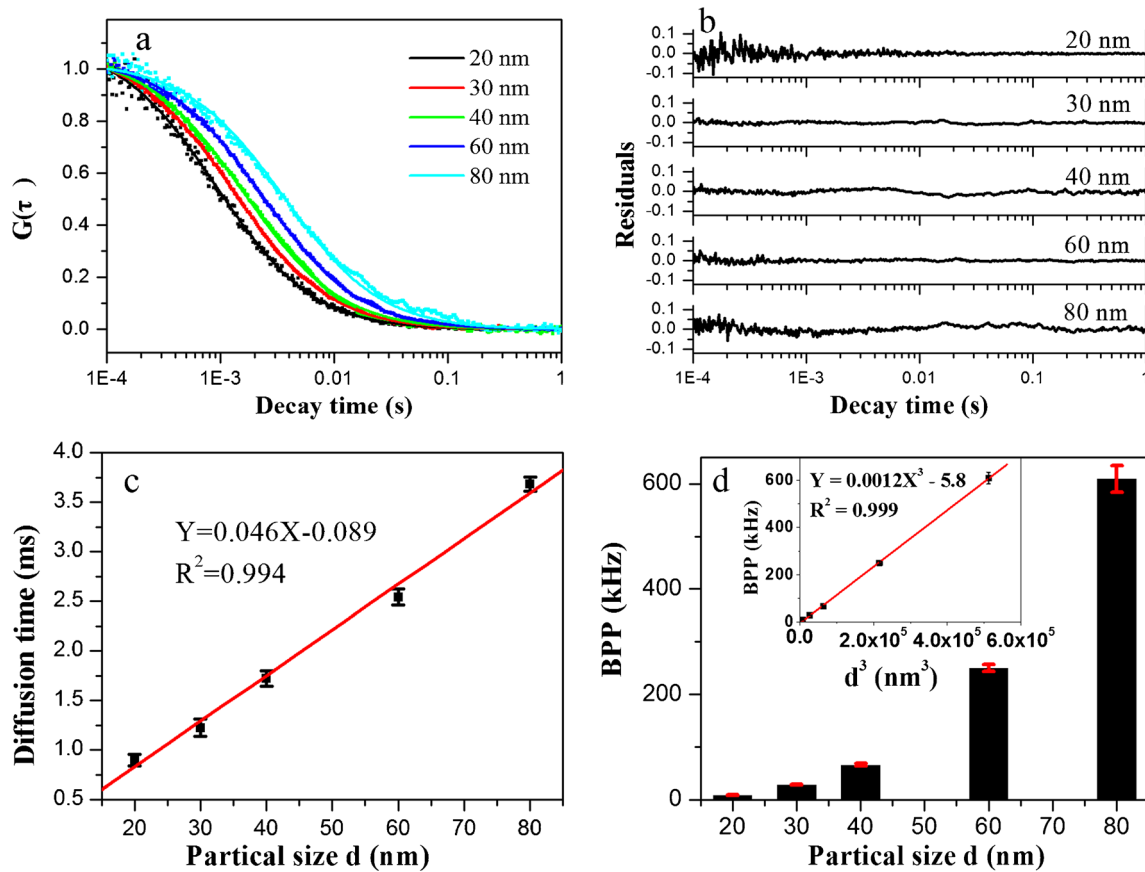


**Fig. 2** Characterization of GNPs by FCS technique. **a** Normalized autocorrelation curves and their fitting curves of GNPs with different sizes. **b** The fitting residual curves of GNPs with different sizes. **c** The linear relationship between the characteristic diffusion time and diameters

of GNPs. **d** The relationship between brightness per particle (BPP) and diameters of GNPs, *inset*: linear relationship between brightness per particle (BPP) and the third power of GNPs' diameters ( $d^3$ ). A series of GNPs (20 nm, 30 nm, 40 nm, 60 nm and 80 nm) were used

aptamer-2 probes and 30  $\mu\text{L}$  buffer (20 mM Tris-HCl with 140 mM NaCl and 10 mM KCl, pH 7.4) were added into a 200  $\mu\text{L}$  polypropylene tube. Then the mixture was incubated at 37  $^\circ\text{C}$  for 1 h. After incubation, FCS measurements of the sample were performed on a home-built FCS system. In the FCS measurements, the recording time per sample was 120 s, and the assay of each sample was repeated three times.

#### Assay of thrombin in human plasma

One hundred  $\mu\text{L}$  of 3.8 % (w/v) sodium citrate solution was added to 900  $\mu\text{L}$  blood, and then the mixture was centrifuged at 3,000 rpm for 15 min. The upper layer was taken out and stored at 4  $^\circ\text{C}$  for immediate use as plasma sample. Thirty  $\mu\text{L}$  of the plasma sample, 120  $\mu\text{L}$  buffer (20 mM Tris-HCl with

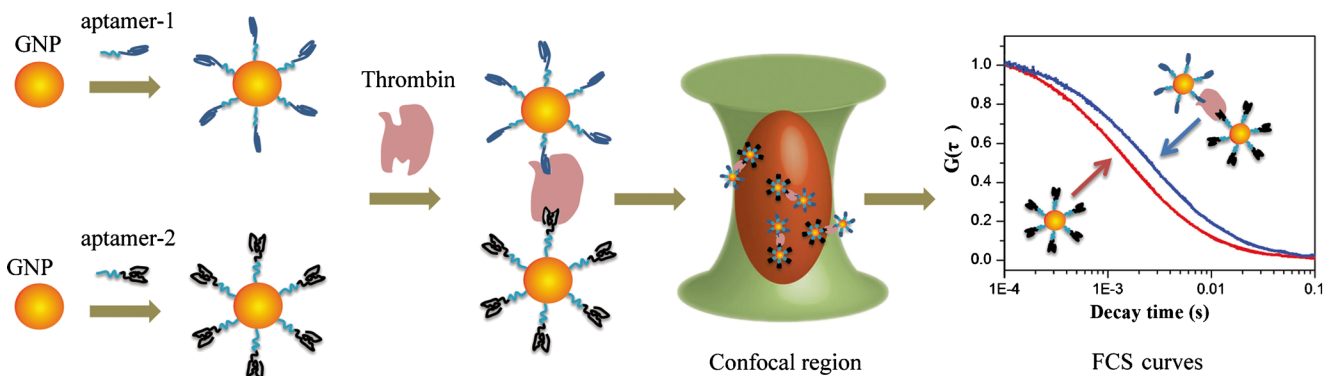
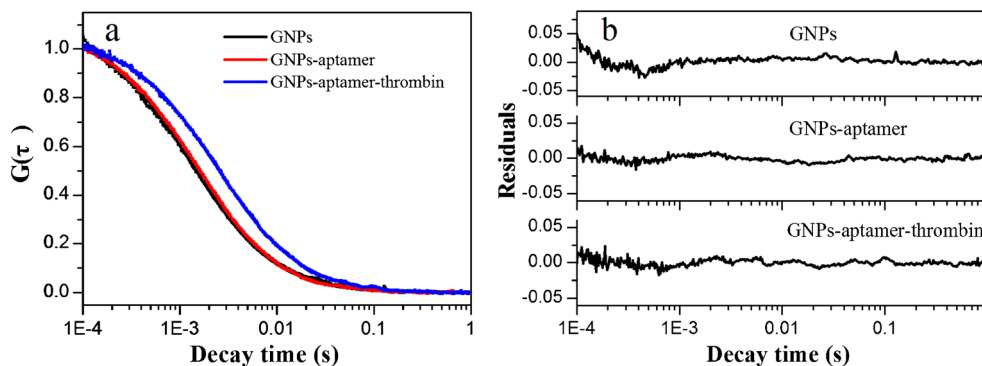


**Fig. 3** Schematic diagram of GNPs-based thrombin assay by fluorescence correlation spectroscopy

**Fig. 4** Normalized autocorrelation curves and their fitting curves of GNPs (340 pM), GNPs-aptamer probes and the mixture after sandwich assay with 110 nM thrombin (a), and their fitting residual curves (b). Thirty nm GNPs were used, and FCS measurement conditions were the same as in Fig. 1a



140 mM NaCl and 10 mM KCl, pH 7.4), 10  $\mu$ L of 0.25 % (w/v) trypsin and 10  $\mu$ L of 32 mM CaCl<sub>2</sub> solution were added into a polypropylene tube. After reaction for 5 min, supernatant of the mixture was taken out and then diluted for assay with the same procedure of assay thrombin, and the final dilution of plasma was 1: 100. Solution of standard thrombin was added to this sample for the recovery assay, and the concentration of the standard thrombin in the sample was 3 nM.

**Results and discussion**

Fluorescent features and diffusion behaviors of GNPs

Figure 1a displays the typical normalized autocorrelation curve of 30 nm GNPs, its fitting curve and fitting residuals. This normalized autocorrelation curve is well fitted with the theoretical mode of autocorrelation function as described in Eq. (1), and the correlation coefficient ( $R^2$ ) is 0.999. The fitting residuals are less than 0.02. This result demonstrates that FCS is a powerful method for investigating the fluorescent

property of GNPs at the single particle level and the fluorescence signal of single GNPs is strong enough to be detected. Figure 1b shows the effects of illumination light intensity on the fluorescent emission of GNPs and fluorescent dyes (Rhodamine B). As shown in Fig. 1b, the emission of GNPs markedly increased with illumination light intensity at low light intensity, and when the illumination light intensity was more than about 3 mW (930 kW cm<sup>-2</sup>) the emission of GNPs basically reached constant, which means the photo-saturation of GNPs in this case. Strictly speaking, in Fig. 1b, the emission of GNPs slowly increased with illumination light intensity over 3 mW, which is mainly attributed to the scattering effects of GNPs. In FCS setup, two emission filters were used to eliminate the scattering effects of GNPs, and in fact, the scattering effects of GNPs can not be completely eliminated. Compared to GNPs, the emission of Rhodamine B markedly increased with illumination light intensity at low light intensity, however, at higher light intensity (more than about 1 mW), the emission of Rhodamine B rapidly decreased with an increase of illumination light intensity due to photobleaching of fluorescent dyes. Compared to organic fluorescent dyes, GNPs show high photo-saturation and no photobleaching features. Figure 2a and b show the normalized

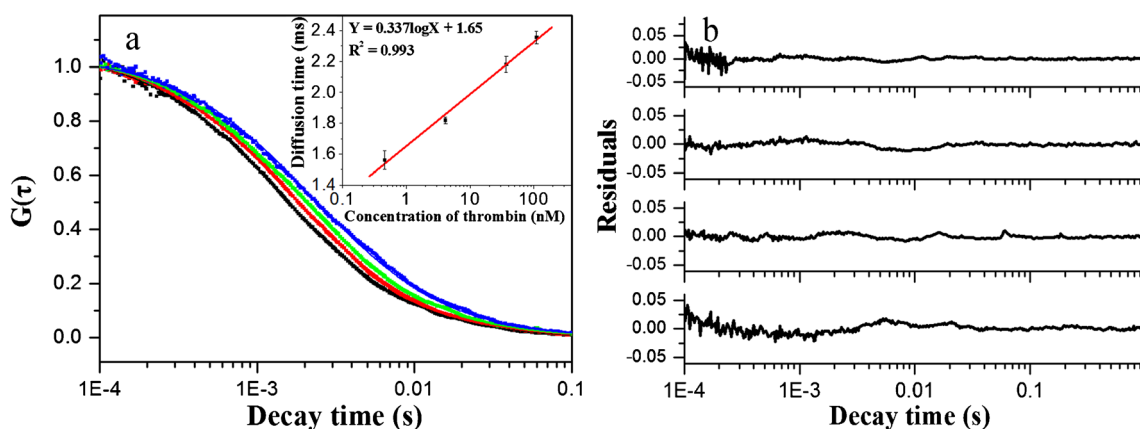


**Fig. 5** a The normalized autocorrelation curves and their fitting curves of GNPs in the different concentration of thrombin, inset: the linear relations between the characteristic diffusion time of GNPs and log thrombin concentration. b The fitting residual curves of GNPs in the

different concentration of thrombin. The 340 pM GNP-aptamers (30 nm) were used to incubate with a series concentrations of thrombin. The FCS measurement conditions were the same as in Fig. 1a

**Table 1** Assay of thrombin in plasma samples and recovery tests

Plasma sample	Thrombin in diluted sample (1:100) (nM)	Thrombin in original sample (nM)	RSD (%) ( $n=3$ )	Thrombin added (nM)	Thrombin found (nM)	Recovery (%)	RSD (%) ( $n=3$ )
1	3.15	315	8.4	3.0	6.01	95.4	9.1
2	3.61	361	5.7	3.0	6.74	104.2	12.6
3	1.73	173	13.7	3.0	4.67	97.7	8.5
4	1.86	186	11.2	3.0	4.64	92.5	7.8

autocorrelation curves of GNPs with different diameters, their fitting curves and fitting residuals. These normalized autocorrelation curves are well fitted with the theoretical mode, and the correlation coefficients ( $R^2$ ) are 0.997–0.999. The fitting residuals are less than 0.1. Figure 2c displays the relationship between the characteristic diffusion times and the GNPs sizes. As shown in Fig. 2c, the characteristic diffusion time linearly increased with an increase of GNPs size, and the correlation coefficient is 0.994, which is in good agreement with Eq. (4). The relative standard deviations (RSDs) of the characteristic diffusion time are less than 7 %. Figure 2d reflects that the relationship between the BPP of GNPs and their sizes. Under a given illumination light intensity, the BPP of GNPs is proportional to the cube of GNP' diameters ( $d^3$ ), which indicated the detection signal was from the fluorescence of GNPs, not from scattering light of GNPs. This is because the fluorescent intensity of GNPs is proportional to the cube of GNP' diameters ( $d^3$ ) and the intensity of the scattering light is proportional to the sixth power of GNP' diameters ( $d^6$ ). Importantly, GNPs possessed a strong BPP despite their low fluorescent quantum yields. For example, the BPP of 40 nm GNPs is more than the BBP of fluorescent dyes such as Rhodamine B at higher illumination light intensity. This result illustrates that GNPs are potential fluorescent labeling probes in bioassay and bioimaging.

#### Principle for FCS assay of thrombin

Thrombin is a trypsin-like serine protease involved in a multitude of processes in the human body, and it can activate neutrophils and platelets which release cytokines, chemotactic factors and growth factors. These processes are associated with inflammation and tissue repair at the blood vessel wall, cardiovascular diseases and certain cancers [29, 30]. Figure 3

shows the principle of thrombin assay using aptamer functionalized GNPs probes, which resembles a sandwich immunoassay. Aptamers are nucleic acids that can bind specific protein sequences, similar to antibodies [31]. In assay of thrombin, when two different GNPs labeled with aptamers are mixed in a sample containing thrombin, the binding reaction will cause GNPs to form dimers (or oligomers), which leads to a significant increase in the characteristic diffusion time of GNPs in the detection volume. FCS method can sensitively detect the change in the characteristic diffusion time of GNPs before and after binding reactions. The quantitative analysis is based on the relation between the change in the characteristic diffusion time of GNPs and the concentration of thrombin.

#### Conjugation of GNPs with aptamers and optimization of experimental conditions

The aptamers for thrombin were prepared according to the references [32, 33] and their sequences were shown in the “Experimental” section. Thiol-capped aptamers were conjugated to GNPs via the Au-S bond, which was shown in Fig. 3. FCS was used for the characterization of GNPs-aptamer conjugates. Initially, five different size GNPs (20, 30, 40, 60 and 80 nm) were chosen as aptamer labeling probes. Since 20 nm GNPs have weaker fluorescence and larger GNPs (40, 60 and 80 nm) modified with aptamer are not very stable in assay of thrombin, only 30 nm GNPs were used in this study.

Figure 4 shows the normalized autocorrelation curves of GNPs, GNPs-aptamer and GNP-aptamer-thrombin-aptamer-GNP complexes (GNP-thrombin complexes). As seen in Fig. 4, the characteristic diffusion time of GNPs-aptamer is larger than that of GNPs, which illustrates that aptamer are successfully conjugated to GNPs' surface. Furthermore, the

**Table 2** Comparison of our method with other methods

Methods	Chemicals	Analytical ranges	Ref.
Fluorescence	Magnetic beads and quantum dots	0.2 nM–4 nM	[22]
SERS	Crystal violet	0.1 nM–10 nM	[23]
Electrochemistry	GNPs and biotin	1 pM–0.1 nM	[24]
FCS	GNPs	0.5 nM–110 nM	This work

characteristic diffusion time of GNP-thrombin complexes is markedly different from that of GNPs, which illustrates that FCS can be used to sensitively detect the change in the characteristic diffusion time of GNPs before and after binding reactions.

We investigated the effects of GNP-aptamer concentration on the binding reaction. As shown in the [electronic supplementary material](#), in the presence of three different concentrations of GNP-aptamer (100 pM, 340 pM, 1,000 pM), the characteristic diffusion time of GNPs also linearly increased with an increase of thrombin concentration. The maximum slope of the curves is in the presence of 340 pM GNP-aptamer. In other words, the sensitivity of the assay is the best in this case. Therefore, 340 pM GNP-aptamer solution was used in subsequent experiments.

### FCS assay of thrombin

Figure 5a shows the normalized autocorrelation curves of GNPs, their fitting curves and fitting residuals under different concentrations of standard thrombin. The results illustrated that normalized autocorrelation curves of GNPs were well fitted by Eq. (1), the correlation coefficients ( $R^2$ ) were from 0.998 to 0.999 and the fitting residuals were less than 0.05. The inset reflects a good linear relation between the characteristic diffusion time of GNPs and log thrombin concentration. The calibration curve of thrombin has a wide linear range over two orders of magnitude (from 0.5 nM to 110 nM), and the detection limit is 0.5 nM for thrombin. This method was successfully applied for direct determination of thrombin level in human plasma. In measurements, plasma samples were 100 times diluted with buffer, and the results are shown in Table 1. As shown in Table 1, the RSDs were from 5.7 % to 13.7 %. The measurement results of thrombin are basically in agreement with the reference [34, 35]. As shown in Table 1, the recoveries of this method were from 92.5 % to 104.2 %, which further illustrated that our method described here was reliable. A comparison with other methods for the determination of thrombin is listed in Table 2.

### Conclusion

We described here the fluorescent properties and diffusion behaviors of GNPs at the single particle level by FCS method. We found that GNPs showed a high photo-saturation feature, and under illumination of stronger light, they possessed no photobleaching and stronger BPP over fluorescent dyes despite their low fluorescent quantum yields. Our results document that GNPs are potential fluorescent labeling probes in bioassay and bioimaging. On the basis of FCS and recognition of aptamers, we developed a new, sensitive and homogenous method for determination of thrombin using GNPs as

fluorescent labeling probes. This new method was successfully applied for direct determination of thrombin levels in human plasma. Compared to current methods, our method is sensitive, rapid, and small sample and reagent requirements, and can expand to homogenous immunoassays and DNA hybridization detection.

**Acknowledgments** We gratefully acknowledge the supports of NSFC (21075081, 20975067, 20905048, 21135004), National Basic Research Program of China (2009CB930400). We also thank Miss Yao Lu for her assistant in conjugation of GNPs with aptamers.

### References

- Weiss S (1999) Fluorescence spectroscopy of single biomolecules. *Science* 283(5408):1676–1683
- Chan WC, Nie S (1998) Quantum dot bioconjugates for ultrasensitive nonisotopic detection. *Science* 281(5385):2016–2018
- Ye C, Wang Y, Li C, Yu J, Hu Y (2013) Preparation of liposomes loaded with quantum dots, fluorescence resonance energy transfer studies, and near-infrared in-vivo imaging of mouse tissue. *Microchim Acta* 180(1–2):117–125
- Huang X, Ren J (2012) Nanomaterial-based chemiluminescence resonance energy transfer: a strategy to develop new analytical methods. *Trac Trends Anal Chem* 40:77–89
- Resch-Genger U, Grabolle M, Cavaliere-Jaricot S, Nitschke R, Nann T (2008) Quantum dots versus organic dyes as fluorescent labels. *Nat Methods* 5(9):763–775
- Shiohara A, Hoshino A, Hanaki K-I, Suzuki K, Yamamoto K (2004) On the cyto-toxicity caused by quantum dots. *Microbiol Immunol* 48(9):669–675
- Peyser LA, Vinson AE, Bartko AP, Dickson RM (2001) Photoactivated fluorescence from individual silver nanoclusters. *Science* 291(5501):103–106
- Lu Y, Huang X, Ren J (2013) Sandwich immunoassay for alpha-fetoprotein in human sera using gold nanoparticle and magnetic bead labels along with resonance Rayleigh scattering readout. *Microchim Acta* 180(7–8):635–642
- Huang CC, Yang Z, Lee KH, Chang HT (2007) Synthesis of highly fluorescent gold nanoparticles for sensing mercury (II). *Angew Chem* 119(36):6948–6952
- Mei Z, Deng Y, Chu H, Xue F, Zhong Y, Wu J, Yang H, Wang Z, Zheng L, Chen W (2013) Immunochromatographic lateral flow strip for on-site detection of bisphenol A. *Microchim Acta* 180(3–4):279–285
- Storhoff JJ, Lucas AD, Garimella V, Bao YP, Müller UR (2004) Homogeneous detection of unamplified genomic DNA sequences based on colorimetric scatter of gold nanoparticle probes. *Nat Biotechnol* 22(7):883–887
- Patra HK, Banerjee S, Chaudhuri U, Lahiri P, Dasgupta AK (2007) Cell selective response to gold nanoparticles. *Nanomed-Nanotechnol* 3(2):111–119
- Tcherniak A, Dominguez-Medina S, Chang W-S, Swanglap P, Slaughter LS, Landes CF, Link S (2011) One-photon plasmon luminescence and its application to correlation spectroscopy as a probe for rotational and translational dynamics of gold nanorods. *J Phys Chem C* 115(32):15938–15949
- Saha K, Agasti SS, Kim C, Li X, Rotello VM (2012) Gold nanoparticles in chemical and biological sensing. *Chem Rev* 112(5):2739–2779
- Gaiduk A, Yorulmaz M, Orrit M (2011) Correlated absorption and photoluminescence of single gold nanoparticles. *ChemPhysChem* 12(8):1536–1541

16. Geddes CD, Parfenov A, Gryczynski I, Lakowicz JR (2003) Luminescent blinking of gold nanoparticles. *Chem Phys Lett* 380(3):269–272
17. Loumagne M, Vasanthakumar P, Lombardi A, Richard A, Débarre A (2013) One-photon excited luminescence of single gold particles diffusing in solution under pulsed illumination. *Phys Chem Chem Phys* 15:4154–4162
18. Chen J, Irudayaraj J (2009) Quantitative investigation of compartmentalized dynamics of ErbB2 targeting gold nanorods in live cells by single molecule spectroscopy. *ACS Nano* 3(12):4071–4079
19. Fang Y, Chang W-S, Willingham B, Swanglap P, Dominguez-Medina S, Link S (2012) Plasmon emission quantum yield of single gold nanorods as a function of aspect ratio. *ACS Nano* 6(8):7177–7184
20. Goldys EM, Sobhan MA (2012) Fluorescence of colloidal gold nanoparticles is controlled by the surface adsorbate. *Adv Funct Mater* 22(9):1906–1913
21. He H, Xie C, Ren J (2008) Nonbleaching fluorescence of gold nanoparticles and its applications in cancer cell imaging. *Anal Chem* 80(15):5951–5957
22. Wang X, Zhao Q (2012) A fluorescent sandwich assay for thrombin using aptamer modified magnetic beads and quantum dots. *Microchim Acta* 178(3–4):349–355
23. Hu J, Zheng P-C, Jiang J-H, Shen G-L, Yu R-Q, Liu G-K (2008) Electrostatic interaction based approach to thrombin detection by surface-enhanced Raman spectroscopy. *Anal Chem* 81(1):87–93
24. Wang H, Liu Y, Liu C, Huang J, Yang P, Liu B (2010) Microfluidic chip-based aptasensor for amplified electrochemical detection of human thrombin. *Electrochem Commun* 12(2):258–261
25. Dong C, Qian H, Fang N, Ren J (2006) Study of fluorescence quenching and dialysis process of CdTe quantum dots, using ensemble techniques and fluorescence correlation spectroscopy. *J Phys Chem B* 110(23):11069–11075
26. Haustein E, Schwille P (2007) Fluorescence correlation spectroscopy: novel variations of an established technique. *Annu Rev Biophys Biomol Struct* 36:151–169
27. Freeman RG, Hommer MB, Grabar KC, Jackson MA, Natan MJ (1996) Ag-clad Au nanoparticles: novel aggregation, optical, and surface-enhanced Raman scattering properties. *J Phys Chem* 100(2):718–724
28. Xu CS, Cang H, Montiel D, Yang H (2007) Rapid and quantitative sizing of nanoparticles using three-dimensional single-particle tracking. *J Phys Chem C* 111(1):32–35
29. Bowman LJ, Anderson CD, Chapman WC (2010) Topical recombinant human thrombin in surgical hemostasis. *Semin Thromb Hemost* 36:477–484
30. Even-Ram S, Uziely B, Cohen P, Grisaru-Granovsky S, Maoz M, Ginzburg Y, Reich R, Vlodaysky I, Bar-Shavit R (1998) Thrombin receptor overexpression in malignant and physiological invasion processes. *Nat Med* 4(8):909–914
31. Jayasena SD (1999) Aptamers: an emerging class of molecules that rival antibodies in diagnostics. *Clin Chem* 45(9):1628–1650
32. Bock LC, Griffin LC, Latham JA, Vermaas EH, Toole JJ (1992) Selection of single-stranded DNA molecules that bind and inhibit human thrombin. *Nature* 355:564–566
33. Tasset DM, Kubik MF, Steiner W (1997) Oligonucleotide inhibitors of human thrombin that bind distinct epitopes. *J Mol Biol* 272(5):688–698
34. Müller J, Becher T, Braunstein J, Berdel P, Gravius S, Rohrbach F, Oldenburg J, Mayer G, Pötzsch B (2011) Profiling of active thrombin in human blood by supramolecular complexes. *Angew Chem Int Ed* 50(27):6075–6078
35. Zhao Q, Li X-F, Le XC (2011) Aptamer capturing of enzymes on magnetic beads to enhance assay specificity and sensitivity. *Anal Chem* 83(24):9234–9236